The Astrophysical Journal, 967:31 (5pp), 2024 May 20 https://doi.org/10.3847/1538-4357/ad3933

Study of the Observation Sensitivity of Gamma-Ray Bursts for the HADAR Project

Zi-hao Zhang[1], Tian-Lu Chen[1], You-Liang Feng[1], Yi-Qing Guo[2,3], Yu-Hua Yao[2,4], Cheng Liu[2], Yang-Zhao Ren[1], Heng-Jiao Liu[1], Hong-Bo Hu[2,3], Qi-Ling Chen[5], Guang-Guang Xin[6], Yi Zhang[7], and Qiang Yuan[7]
[1] The Key Laboratory of Cosmic Rays (Tibet University), Ministry of Education, Lhasa 850000, Tibet, People's Republic of China; chentl@utibet.edu.cn, fengyouliang@utibet.edu.cn
[2] Key Laboratory of Particle Astrophysics, Institute of High Energy Physics, Chinese Academy of Sciences, Beijing 100049, People's Republic of China
[3] University of Chinese Academy of Sciences, 19 A Yuquan Road, Shijingshan District, Beijing 100049, People's Republic of China
[4] College of Physics, Chongqing University, No. 55 Daxuecheng South Road, High-tech District, Chongqing 401331, People's Republic of China
[5] College of Physics, Sichuan University, Chengdu 610064, People's Republic of China
[6] Suzhou Aerospace Information Research Institute, Suzhou 215123, People's Republic of China
[7] Key Laboratory of Dark Matter and Space Astronomy, Purple Mountain Observatory, Chinese Academy of Sciences, Nanjing 210008, People's Republic of China
Received 2024 January 29; accepted 2024 March 29; published 2024 May 15

Abstract

The High Altitude Detection of Astronomical Radiation (HADAR) is a novel wide-field Cherenkov Telescope. It is designed for gamma-ray astronomy in the energy range of 10 GeV to 100 TeV, with gamma-ray bursts (GRBs) being one of its primary research focuses. To assess its complementary capabilities, this study first presents the Crab sensitivity of HADAR. Then, to compare the sensitivity of GRBs, the observation time for all experiments is standardized to 100 s. To clearly demonstrate HADAR's advantages, we estimate its observational results with a 221009A-like GRB. The study found that HADAR is capable of more comprehensively recording the bending and absorption of self-Compton radiation, which is expected to fill observational gaps in space- and ground-based experiments. We anticipate that this facility will ensure a large statistical GRB sample and advance our understanding of GRBs.

Unified Astronomy Thesaurus concepts: Gamma-ray bursts (629); Cosmic rays (329); Gamma-ray telescopes (634)

1. Introduction

Gamma-ray bursts (GRBs) are extremely intense explosions that typically last for a short duration but release a tremendous amount of energy. These phenomena are often associated with extreme astrophysical events such as supernova explosions, the formation of black holes, or mergers of neutron stars, and the release of a concentrated burst of gamma rays. (Panaitescu & Mészáros 1998; Pilla & Loeb 1998; Wei & Lu 1998; Sari & Esin 2001; Zhang & Mészáros 2001; Asano & Inoue 2007; Xue et al. 2009). Studying GRBs is of significant importance for understanding extreme physical processes, interstellar environments, and the origin of cosmic rays. Current research on afterglows and prompt emission has gradually allowed us to build models for the central engine (Sari et al. 1998), burst environment (Lee & Ramirez-Ruiz 2007; Fryer et al. 2019), jet properties, and afterglow radiation (Dichiara et al. 2022) of GRBs. But in the very high energy (VHE), we still need more observation.

Out of the seven high-energy GRBs that have been observed, GRB 221009A's will modify the currently most standard GRB afterglow model by 13 TeV photons energy (The LHAASO Collaboration et al. 2023). The multiband lightcurve and wide spectrum study of GRB 190829A supports the existence of at least two radiation components (H.E.S.S. Collaboration et al. 2021). GRB 190114C proves that the synchrotron self-Compton (SSC) process is one of the mechanisms for producing extremely high-energy photons (MAGIC Collaboration 2019). GRB 180720B indicates that the magnetic field structure is closely related to the physical processes of emission, dissipation, and acceleration of relativistic jets (Abdalla et al. 2019). This indicates that more observations will further promote theoretical development. Therefore, the High Altitude Detection of Astronomical Radiation (HADAR) experiment was proposed: using lens refraction to avoid the field-of-view (FOV) obstruction of reflective telescopes, expanding the detector's FOV through convex lenses, and conducting observations in high-altitude areas to improve the detector's sensitivity (Cai et al. 2017). By increasing the sensitivity, we estimate that the annual observation rate of HADAR will reach 5.8 (Yao et al. 2023).

The experiment is planned to be conducted at the Yangbajing International Cosmic Ray Observatory, located at an altitude of 4300 m (90°.522E, 30°.102N, 606 g cm^{-2}). The experiment consists of four atmospheric Cherenkov telescopes, with a 5 m diameter acrylic hemisphere on top to expand the detector's FOV to 60°. These telescopes are mounted on a 7 m high cylindrical water tank and filled with purified water. The imaging module comprises 18,961 photomultiplier tubes (PMTs) with a diameter of 5 cm where, on the bottom of the tank, they are used for imaging the Cherenkov light produced by gamma and cosmic rays in the atmosphere. The team has already completed the engineering prototype experiment in 2015 and successfully observed cosmic-ray events (Chen et al. 2019), and is currently conducting a 2 m diameter pilot experiment. This paper presents relevant simulation studies based on the complete HADAR array, introduces the performance and calculation methods in Section 2, discusses the expected observations of GRB 221009A in Section 3, and concludes with a discussion in Section 4.

2. Experimental Sensitivity

To evaluate the angular resolution and effective area of HADAR in the 10 GeV to 100 TeV, we used the Cosmic Ray

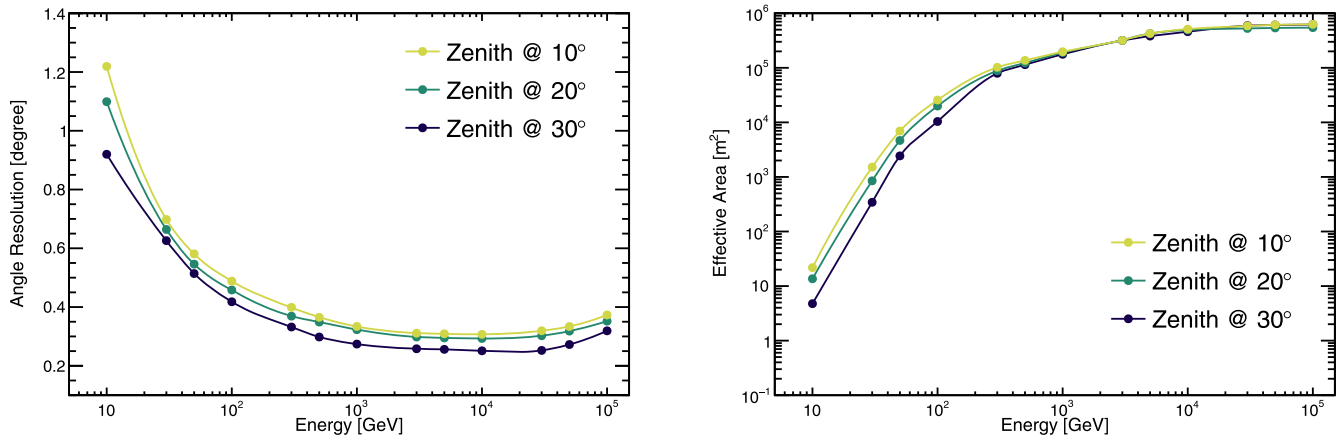

Figure 1. HADAR's observation capabilities for gamma-ray radiation at incident zenith angles of 10°, 20°, and 30°. The left graph is the variation of HADAR's angle resolution with energy. The right graph is the change in the effective area of the HADAR experiment with energy.

Simulations for Kascade (CORSIKA) program to generate a large number of extensive air shower samples, using the QGSJETII-04 and FLUKA models, respectively (Homola et al. 2015), as shown in Figure 1.

We found the angle resolution capability with increasing energy for incidence angles of 10°, 20°, and 30°. At the optimal energy (∼10 TeV) and incidence angle (30°), an angle resolution of 0.°25 for gamma sources was found. We believe this is because events with larger incidence angles and higher energy have more elongated Hillas ellipses on the detector plane, which is more conducive to reconstruction. As the energy continues to increase (>10 TeV), the angle resolution gradually deteriorates to approximately 0.°3–0.°4. We believe this is due to the triggering process, where, in order to reduce contamination from night sky background and starlight, we fixed the triggering window to the size of 10 × 10 pixels of the PMT (Xin et al. 2022), considering only the distribution and counting of photons within the triggering window, leading to incomplete imaging and degraded reconstruction for high-energy events. This triggering method does not fully utilize the advantage of HADAR's large imaging area. Therefore, we are considering the use of dynamically adjusting the triggering window, and related simulation work is currently underway. From the right figure, we observe that HADAR's effective area rapidly increases from 10 m^2 to over 10^5 m^2 with increasing energy for different zenith angle incidences. After 10 TeV, the effective area no longer undergoes significant changes due to the stabilization of the reconstruction success rate.

The Crab Nebula is a remnant of a supernova explosion. The gamma-ray emission from the Crab Nebula is very stable, and therefore astronomers also refer to the Crab Nebula as the "standard candle." Astronomers characterize the detector's ability to detect other faint sources by estimating the sensitivity of the detector to the standard candle. HADAR's significance estimation for the Crab Nebula is calculated based on the Li–Ma formula (Li & Ma 1983):

$$S[i] = \frac{N'_\gamma[i]}{\sqrt{N_{\rm CR}[i]}} = \frac{N_\gamma[i]}{\sqrt{N_{\rm CR}[i]}} \times W.$$

$N_\gamma[i]$ and $N_{\rm CR}[i]$ are the numbers of photons and protons collected by HADAR at energy i during a certain period of observation time. The annual estimated observation time of HADAR for the Crab Nebula is 380 hr (solar zenith angle >108°, lunar zenith angle >80°), and they are calculated by the following equations:

$$N_\gamma[i] = T_{\rm obs} \times S_E \times F_{\rm sample,crab} \times \frac{N_{\gamma,\rm sim}[i]}{N_{\gamma,\rm sim,all}[i]} \times Q_E[i] \times \epsilon_\gamma$$

$$N_{\rm CR}[i] = T_{\rm obs} \times S_E \times F_{\rm sample,CR} \times \frac{N_{\rm CR,sim}[i]}{N_{\rm CR,sim,all}[i]} \times \Omega_E[i].$$

ϵ_γ is the ratio of gamma-ray-to-total events within the angle resolution, which is taken as 68% in this paper. The number of photons $N_\gamma[i]$ is the product of the simulated integral flux sample from CORSIKA, the scatter area S_E, the Q_E ability γ/p, the reconstruction success rate $N_{\gamma,\rm sim}[i]/N_{\gamma,\rm sim,all}[i]$, and the observation time $T_{\rm obs}$; the same applies to the number of protons. In the CORSIKA simulation, gamma rays and cosmic rays are generated according to a power law with a spectral index of −2.7, which does not accurately reflect the gamma-ray flux of the Crab Nebula (The LHAASO Collaboration et al. 2021). Therefore, W is introduced to correct the number of generated particles to the actual observed particle number $N'_\gamma[i]$:

$$W = \frac{(E/\rm TeV)^{-2.479-2.069\times\log\left(\frac{E}{\rm TeV}\right)}}{(E/\rm TeV)^{-2.7}}$$

$$N'_\gamma[i] = W \times N_\gamma[i].$$

W is the ratio of the spectral index of the fitted spectrum of the Crab Nebula in the observation energy range to the simulated spectral index from CORSIKA. The fitted spectrum is a log-parabola function. The true spectral index and the simulated spectral index of protons within the observation energy range are both approximately −2.7, so no correction is necessary. Therefore, the integral sensitivity $F_{\rm sensitivity}$ at energy i is:

$$\frac{F_{\rm sensitivity}}{F_{\rm crab}} = \frac{5}{S[i]},$$

$$F_{\rm crab} = \int_i^\infty 3.902 \times 10^{-11} \times \left(\frac{E}{\rm TeV}\right)^\alpha ({\rm TeV^{-1}\,cm^{-2}\,s^{-1}})dE,$$

$$\alpha = -2.479\text{–}0.2069 \times \log\left(\frac{E}{\rm TeV}\right).$$

We find that the annual observation sensitivity of the experiment is below $1\%I_{\rm crab}$ near 1 TeV, which is lower than

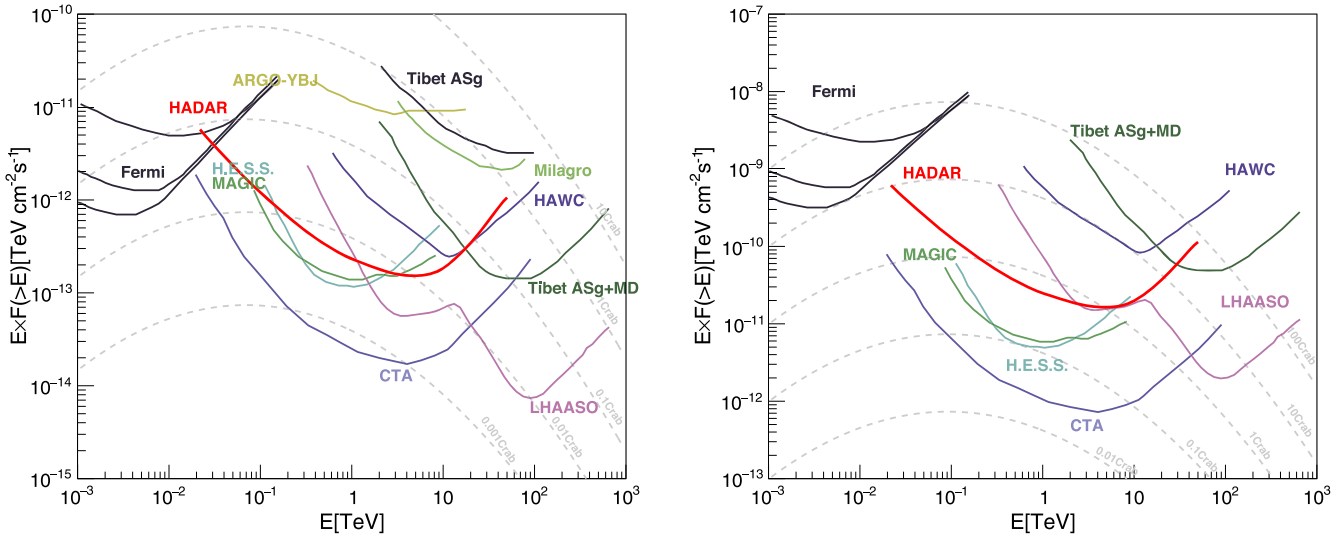

Figure 2. The left graph shows the annual integral sensitivity of the HADAR experiment compared to other experiments for the Crab Nebula. The Fermi experiment is represented by three lines from top to bottom corresponding to 4 yr of observation time at positions ($l = 0°$, $b = 0°$), ($l = 0°$, $b = 30°$), and ($l = 0°$, $b = 90°$) (Bregeon et al. 2013); HESS (De Angelis et al. 2008), MAGIC (dual-mirror joint observation; Aleksić et al. 2016), VERITAS (De Angelis et al. 2008), CTA (Acharya et al. 2013; Maier et al. 2017) for 50 hr of observation time; Tibet ASγ+MD (Huang 2011) with 3278 hr of observation time, Milagro (DeYoung et al. 2012), ARGO-YBJ (Bartoli et al. 2013), HAWC (DeYoung et al. 2012; Mostafá & Collaboration 2014), LHAASO (Cao et al. 2014) for 1 yr of observation time; the right graph shows the integral sensitivity comparison of all experiments for the Crab Nebula within 100 s of observation time.

that of LHAASO-WCDA, HESS, and MAGIC. At higher energies (>3 TeV), it outperforms HESS and MAGIC, and is comparable to HAWC in Figure 2; at lower energies (<100 GeV), it can still observe fluxes lower than $10\%I_{\rm crab}$, which is better than HESS and MAGIC. Due to differences in the geographical locations and implementations of different experiments, the observation times for the Crab Nebula are not uniform across experiments. For the statistical discovery of the burst duration T_{90}, which is found to be mostly less than 100 s (Qin et al. 2012), we adjust the observation time $T_{\rm obs}$ to a standardized value of $T'_{\rm obs} = 100$ s to compare these experiments' observational capabilities for transient sources

$$F'_{\rm sensitivity} = F_{\rm sensitivity} \times \sqrt{\frac{T'_{\rm obs}}{T_{\rm obs}}}.$$

It can be observed that at around 1 TeV, HADAR is still able to observe fluxes lower than $1I_{\rm crab}$ in Figure 2 (left). At higher energy ranges (>2 TeV), HADAR's sensitivity is comparable to or better than LHAASO-WCDA, and superior to HAWC; at lower energy, it is better than LHAASO-WCDA. Although HADAR's sensitivity within an observation time of 100 s is still lower than that of MAGIC and HESS, the wide FOV advantage of HADAR allows it to fully record all transient events within its FOV, which narrow FOV telescopes like MAGIC and HESS cannot achieve. Therefore, we believe that relying on its advantages of wide FOV and low-energy sensitivity, HADAR can conduct comprehensive observations of transient sources with relatively sensitive accuracy.

3. Expected Observations of GRB 221009A

GRB 221009A is a rare and unique GRB, being the brightest ever observed since the first discovery of GRBs by humans. The energy released in this event even exceeds that of the second brightest GRB in the Fermi catalog by a factor of 15 (Stern & Tkachev 2023). The duration of this burst also extends to 1000 s, during which almost all space- and ground-based detectors captured the photons emitted by it. For example, HXMT and GECAM (An et al. 2023), Fermi, Swift (Williams et al. 2023), and LHAASO recorded the burst and its afterglow in the several hundred GeV to several TeV range (LHAASO Collaboration et al. 2023). The event was first recorded by the Fermi Gamma-ray Burst Monitor (GBM) on 2022 October 9, at 13:16:59.988 UT and marked as the T_0 moment for GRB 221009A (Lesage et al. 2022). Through analysis, the burst exhibits many unique features, such as a relatively close redshift of $z = 0.151$, a high isotropic energy of 1.5×10^{55} erg (Abdo et al. 2009), and an extremely narrow jet half-opening angle of 0°.8 (LHAASO Collaboration et al. 2023). Astronomers generally believe that GRB jets have a certain angle, with the core region being much brighter than other areas, so the apparent brightness of GRBs depends on the observer's viewing angle relative to the jet and its intrinsic energy (Dai & Gou 2001; Rossi et al. 2002; Zhang & Meszaros 2002). This indicates that, under the theoretical assumptions of jet structure, GRB 221009A is an extremely special event.

In previous work, we estimated using Fermi data that HADAR's annual observation rate for GRBs could reach 5.8 events per year (Yao et al. 2023). Therefore, we can assume that the T_0 moment of GRB 221009A coincidentally occurs within the FOV of HADAR. In Figure 3, HADAR can not only record the instantaneous radiation completely but also conduct relevant follow-up observations over a time span of 1000 s. Therefore, using the SSC radiation model assumption (Wang et al. 2019), the theoretical spectrum of GRB 221009A at 230–300 s was provided, and the expected observational spectrum was obtained based on the model and effective area. It was found that HADAR can capture more spectrum details, including the bend in the synchrotron radiation phase and high-energy absorption, with smaller observational errors.

In addition to the energy spectrum, scientists also gain further understanding of GRBs by analyzing the distribution of photon energy and arrival time, which requires detectors to be able to fully record the variability of light. In Figure 4, the low-energy transient radiation process of GRB 220910A caused varying degrees of saturation effects on HXMT, LAT, and

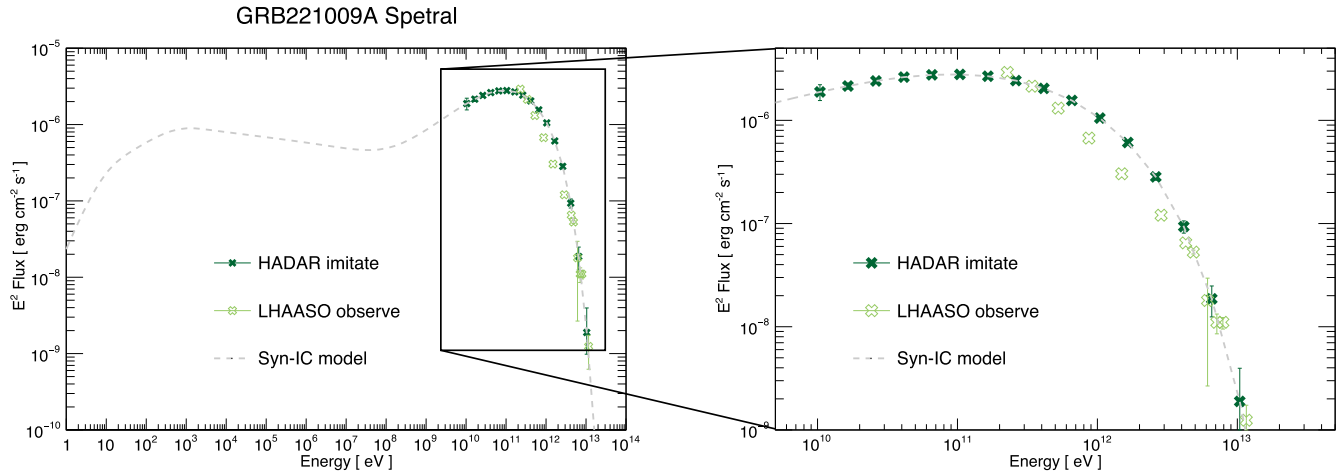

Figure 3. SSC model, LHAASO-WCDA observation results (The LHAASO Collaboration et al. 2023), and the expected observations of HADAR.

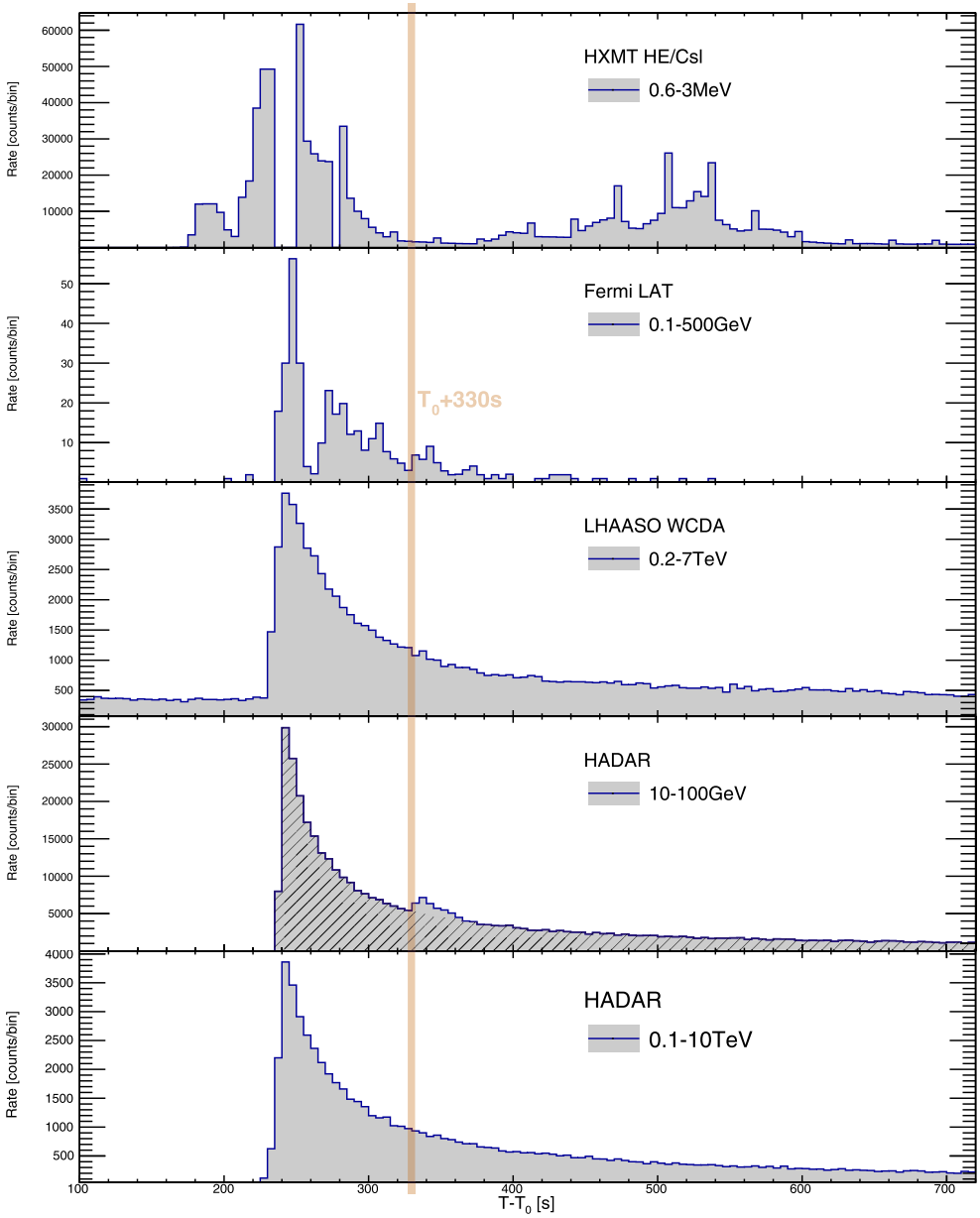

Figure 4. HXMT (An et al. 2023), Fermi-LAT (Bissaldi et al. 2023), and LHAASO-WCDA (The LHAASO Collaboration et al. 2023) have observed the lightcurve of GRB 221009A, and HADAR has predicted observations in the energy ranges of 10–100 GeV and 0.1–10 TeV, with a bin width of 5 s.

GBM (An et al. 2023; Bissaldi et al. 2023). Additionally, due to Fermi's orbit and FOV limitations, no further recording was possible after $T_0 + 435$ s. At high energies, LHAASO-WCDA recorded approximately 64,000 photons but was unable to observe the fine structure of the lightcurve (The LHAASO Collaboration et al. 2023). The broad spectral coverage provided by HADAR allows us to constrain the energy of reconstructed photons and to separately consider the verification of the SSC radiation, particularly necessitating a comprehensive recording of low-energy photons. We found that in the energy ranges of 10–100 GeV and 0.1–10 TeV, HADAR could collect approximately 763,000 and 58,300 photons, respectively, within $<T_0 + 1000$ s, leveraging HADAR's observational advantages. Furthermore, HADAR recorded the main pulse at $T_0 + 240$ s and the second pulse at $T_0 + 330$ s, with the second pulse typically considered the beginning of the afterglow deceleration. The bulk Lorentz factor Γ of GRB is calculated based on the afterglow onset time (Lesage et al. 2023).

4. Summary

With the advent of imaging atmospheric Cherenkov telescopes such as HESS and MAGIC, gamma-ray astronomy has achieved remarkable success. HADAR will focus on VHE observations aiming to improve the insufficient observational capabilities for transient sources through its large FOV and high sensitivity advantages. To clearly assess the performance of HADAR, we simulated the array of all detectors. We found that the angular resolution of HADAR improves with increasing energy and incident angle, reaching an optimal level of $0.^{\circ}25$ at around TeV. The effective area increases rapidly at lower energies, reaching 10^6 m^2 after TeV. Therefore, we estimate that HADAR's crab sensitivity is comparable to LHAASO, HESS, and MAGIC at TeV.

GRBs are an important topic for HADAR. In order to uniformly evaluate the GRB sensitivity of each experiment, we standardized the observation time to 100 s. We found that HADAR fills the observational gaps of satellite and ground-based experiments with good sensitivity, which is very beneficial for fully recording the burst process of GRBs. In addition, through simulating the energy spectrum and lightcurve of the well-known GRB 221009A, we found that HADAR comprehensively recorded the self-Compton radiation bend ($\sim$100 GeV) and absorption, which is crucial for understanding the physics behind the GRB spectrum. We also found that HADAR could record approximately 763,000 photons during the burst and, like Fermi, record the second pulse in the 10–100 GeV energy range, which is important for estimating the redshift of GRBs. This indicates that HADAR has the capability to more comprehensively record the burst information of GRBs, demonstrating its unique observational potential in the domain of very high-energy transient astronomy.

Acknowledgments

This work is supported by the National Natural Science Foundation of China (No. 12275279) and Central Government Funds for Local Scientific and Technological Development (grant No. JDRC2023000009), and Natural Science Foundation of Tibet Autonomous Region (grant No. ZRKX2024000092).

ORCID iDs

Zi-hao Zhang https://orcid.org/0000-0002-0786-7307
Tian-Lu Chen https://orcid.org/0000-0002-2944-2422
Yi-Qing Guo https://orcid.org/0000-0003-4932-9619
Yu-Hua Yao https://orcid.org/0000-0002-4611-0075
Qiang Yuan https://orcid.org/0000-0003-4891-3186

References

Abdalla, H., Adam, R., Aharonian, F., et al. 2019, Natur, 575, 464
Abdo, A. A., Ackermann, M., Arimoto, M., et al. 2009, Sci, 323, 1688
Acharya, B., Actis, M., Aghajani, T., et al. 2013, APh, 43, 3
Aleksić, J., Ansoldi, S., Antonelli, L. A., et al. 2016, APh, 72, 76
An, Z.-H., Antier, S., Bi, X.-Z., et al. 2023, arXiv:2303.01203
Asano, K., & Inoue, S. 2007, ApJ, 671, 645
Bartoli, B., Bernardini, P., Bi, X., et al. 2013, ApJ, 779, 27
Bissaldi, E., Bruel, P., Omodei, N., Pillera, R., & Di Lalla, N. 2023, ICRC (Nagoya), 444, 847
Bregeon, J., Charles, E., & Wood, M. 2013, arXiv:1304.5456
Cai, H., Zhang, Y., Liu, C., et al. 2017, JInst, 12, P09023
Cao, Z. 2014, NIMPA, 742, 95
Chen, T., Liu, C., Gao, Q., et al. 2019, NIMPA, 927, 46
Dai, Z., & Gou, L. 2001, ApJ, 552, 72
De Angelis, A., Mansutti, O., & Persic, M. 2008, NCimR, 31, 187
DeYoung, T. 2012, NIMPA, 692, 72
Dichiara, S., Troja, E., Lipunov, V., et al. 2022, MNRAS, 512, 2337
Fryer, C. L., Lloyd-Ronning, N., Wollaeger, R., et al. 2019, EPJA, 55, 1
H.E.S.S. Collaboration, Abdalla, H., Aharonian, F., et al. 2021, Sci, 372, 1081
Homola, P., Engel, R., & Wilczyński, H. 2015, APh, 60, 47
Huang, J. 2011, ICRC (Beijing), 11, 107
Lee, W. H., & Ramirez-Ruiz, E. 2007, NJPh, 9, 17
Lesage, S., Veres, P., Briggs, M., et al. 2023, ApJL, 952, L42
Lesage, S., Veres, P., Roberts, O., et al. 2022, GCN, 32642, 1
LHAASO Collaboration, Cao, Z., Aharonian, F., et al. 2023, Sci, 380, 1390
Li, T.-P., & Ma, Y.-Q. 1983, ApJ, 272, 317
MAGIC Collaboration 2019, Natur, 575, 455
Maier, G., Arrabito, L., Bernlöhr, K., et al. 2017, ICRC (Busan), 301, 846
Mostafá, M. A. 2014, BrJPh, 44, 571
Panaitescu, A. D., & Mészáros, P. 1998, ApJ, 501, 772
Pilla, R. P., & Loeb, A. 1998, ApJL, 494, L167
Qin, Y., Liang, E.-W., Liang, Y.-F., et al. 2012, ApJ, 763, 15
Rossi, E., Lazzati, D., & Rees, M. J. 2002, MNRAS, 332, 945
Sari, R., & Esin, A. A. 2001, ApJ, 548, 787
Sari, R., Piran, T., Narayan, R., et al. 1998, ApJL, 497, L17
Stern, B., & Tkachev, I. 2023, JETPL, 118, 553
The LHAASO Collaboration, Cao, Z., Aharonian, F., et al. 2021, Sci, 373, 425
The LHAASO Collaboration, Cao, Z., Aharonian, F., et al. 2023, SciA, 9, eadj2778
Wang, X.-Y., Liu, R.-Y., Zhang, H.-M., Xi, S.-Q., & Zhang, B. 2019, ApJ, 884, 117
Wei, D., & Lu, T. 1998, ApJ, 505, 252
Williams, M. A., Kennea, J. A., Dichiara, S., et al. 2023, ApJL, 946, L24
Xin, G.-G., Cai, H., Guo, Y.-Q., et al. 2022, NuScT, 33, 25
Xue, R., Tam, P., Wagner, S., et al. 2009, ApJ, 703, 60
Yao, Y.-H., Wang, Z., Chen, S., et al. 2023, ApJ, 958, 87
Zhang, B., & Mészáros, P. 2001, ApJ, 559, 110
Zhang, B., & Meszaros, P. 2002, ApJ, 571, 876